ARTICLES

Fast Photodynamics of Aqueous Formic Acid

Jan Thøgersen, Svend Knak Jensen, Ove Christiansen, and Søren R. Keiding*

Department of Chemistry, University of Aarhus, Langelandsgade 140, DK 8000 Århus C, Denmark

Received: March 31, 2004; In Final Form: July 15, 2004

Femtosecond transient absorption spectroscopy is used to investigate the primary reaction dynamics of aqueous formic acid, HCOOH(aq), following the photoexcitation of the n → π^* transition at 200 nm. Using probe pulses covering the spectral range from 200 to 620 nm, we find that the only detectable photoproduct is the OH radical, which suggests that HCOOH(aq) dissociates predominantly into the HCO + OH channel. The absence of signals assignable to the formyl radical is discussed, and the properties of hydrated formyl radicals are investigated using high-level electronic structure calculations.

I. Introduction

In this work, we report an investigation of the primary photochemistry of aqueous formic acid using femtosecond transient absorption spectroscopy. The n → π^* transition of the carbonyl group is common to all carboxyl acids, and the photolysis of this entity thus is relevant for a large number of organic molecules. As an important example, excitation of the n → π^* transition in simple amino acids with circularly polarized light has been invoked to explain the puzzling homochirality of amino acids in biological systems.[1] Further studies of this hypothesis necessitate a detailed knowledge of the primary photochemistry of amino acids in both the gaseous and aqueous phases. Preliminary studies in our group of the primary photochemistry of aqueous alanine indicate that the photolysis of a simple amino acid is rather complicated. Hence, in an attempt to simplify the analysis of the alanine photochemistry, we start by investigating only the carboxylic part, that is, by studying the photochemistry of aqueous formic acid.

Only little is known about the primary photolysis of aqueous HCOOH. As many of the expected photoproducts are highly reactive in the aqueous environment, previous experimental investigations with low time resolution have shown not only the primary photochemistry, but also secondary or tertiary reactions induced by the photoproducts. The occurrence of secondary reactions among the photoproducts is also suggested by the concentration dependencies observed. However, both Adams et al.[2] and Karpel et al.[3] suggest that the reaction HCOOH(aq) + $\hbar\omega$ → HCO(aq) + OH(aq) is the primary photolytic decomposition of formic acid when excited with continuous wave light sources at 253.7 or 184.9 nm. In contrast to the scarce literature on the photochemistry of HCOOH(aq), the experimental and theoretical studies of gas-phase HCOOH photodissociation are rather comprehensive. A recent theoretical study[4] of the photodissociation dynamics gives a good overview of the experimental and theoretical work performed on gas-phase HCOOH: The ground state S_0 (X^1A') of gas-phase HCOOH is planar, and the C═O carbonyl bond is the chromophore. The lowest excited singlet state corresponds to excitation from the nonbonding orbital on the carbonyl oxygen atom to the antibonding carbonyl π^* orbital. The analogous n → π^* excitation of formaldehyde is symmetry forbidden, and accordingly, in HCOOH, the n → π^* transition is rather weak with a band maximum in the gas phase at 215 nm. Excitation of the n → π^* band leads to wavelength-dependent dissociation into five different channels.[5−10] These are listed in Table 1, along with the calculated heats of reaction[4,5,10] and selected reaction barriers.[4] The gas-phase investigations indicate that, at short wavelengths (λ < 240 nm), the main product channel is HCO ($^2A'$) + OH ($^2\Pi$). This product channel is accessible from both the lowest excited singlet (S_1) and triplet (T_1) states. Laser-induced fluorescence[8] and REMPI[10] studies have shown that the HCO and OH photoproducts are formed with very little rovibrational energy with the excess energy predominantly appearing as recoil energy.[7] At longer wavelengths ($\lambda \geq$ 240 nm), the two elimination channels H_2 + CO_2 and H_2O + CO become accessible through the internal conversion to the S_0 ground state. These channels are also observed when formic acid is photolyzed in low-temperature rare gas matrixes.[11,12] The two remaining channels, involving the dissociation of an O−H or C−H bond, are observed with small but increasing yields as the energy of the photolysis photon is increased.[9,13] Using the well-known gas-phase photodissociation dynamics as a reference, the photolysis of aqueous formic acid thus also offers an interesting system for elucidating the influence of the solvent on the primary reactivity. In this work, we apply femtosecond

TABLE 1: Gas Phase Dissociation Channels of HCOOH Following Excitation of the n → π^* Band[5−10]

product channel	ΔH° [a] (kJ/mol)	barrier[b] (kJ/mol)	pathway[c]
HCO + OH	431	56	S_1
H + COOH	390	41	T_1
H + HCOO	448	81	S_1
H_2 + CO_2	35	285−300	S_0
H_2O + CO	−6	285−300	S_0

[a] Calculated heat of reaction.[4,5,10] [b] Reaction barrier.[4] [c] Electronic pathway for the dissociation process (S_0, S_1, or T_1) for the corresponding dissociation channel.

* Corresponding author. E-mail: keiding@chem.au.dk.

10.1021/jp048593d CCC: $27.50
Published on Web 08/24/2004

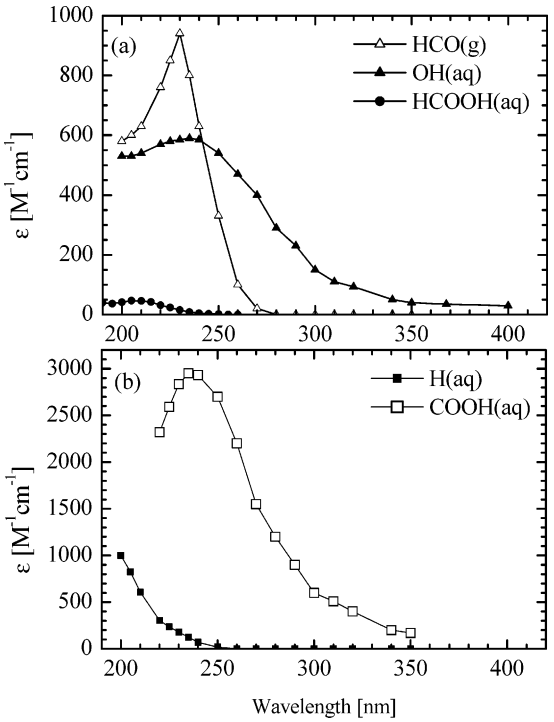

Figure 1. (a) Steady-state absorption spectra of the main photolysis channel in formic acid. The spectrum of the formyl radical (HCO) in the aqueous phase is not known, and the spectrum depicted is the gas-phase spectrum. (b) Steady-state absorption spectra of the possible products H(aq) and COOH/HCOO(aq).[19−22]

transient absorption spectroscopy to measure the primary reaction dynamics of aqueous HCOOH following photoexcitation at 200 nm.

II. Absorption Spectra

The experimental technique of transient absorption spectroscopy identifies the species involved in the photolysis by their absorption spectra. This section presents the steady-state absorption spectra of the primary species involved in the photolysis of aqueous formic acid. The absorption spectrum of HCOOH(aq) recorded by an Agilent 8453 spectrometer with a spectral resolution of 1 nm is shown in Figure 1a. The HCOOH-(aq) absorption maximum, corresponding to an extinction coefficient of $\epsilon = 43 \pm 3\ M^{-1}\ cm^{-1}$, is located at 207 nm. The maximum extinction coefficient is close to that of HCOOH-(g),[14] and the spectral peak is blue shifted by only 8 nm (0.2 eV) relative to the peak position of the gas-phase spectrum. This indicates that hydration is of minor importance to the potential energy surfaces in the Franck−Condon region of the $n \rightarrow \pi^*$ transition. The absorption spectrum of the aqueous hydroxyl radical, OH(aq), is taken from the works of Pagsberg et al.[15] and Boyle et al.[16] It has a maximum extinction coefficient of $590 \pm 80\ M^{-1}\ cm^{-1}$ at 230 nm and extends from below 200 to 350 nm. The gas-phase absorption spectrum of the formyl radical, measured by pulse photolysis, has a weak red absorption band between 450 and 900 nm and a much stronger absorption in the UV part of the spectrum, with a maximum absorption corresponding to $\epsilon = 941 \pm 171\ M^{-1}\ cm^{-1}$ at 230 nm.[17] The absorption spectrum of aqueous HCO has, to the best of our knowledge, not been observed and the existence of HCO(aq) has also been questioned as HCO either could be rapidly hydrated to form $HC(OH)_2$[18] or could dissociate or ionize. This issue will be discussed further later. Also, H(aq), HCOO(aq), and COOH(aq) can potentially contribute to the transient absorption in the spectral range between 200 and 400 nm.[19−22] In the aqueous phase, HCOO(aq) and COOH(aq) have not been separately identified.[20,22] Their spectra are shown in Figure 1b. In addition to the primary photoproducts listed above, the photolysis of aqueous solvent will produce hydrated electrons and possibly also H(aq) and OH(aq).[23,24] These species give rise to a small signal of maximum 5% in the spectral range investigated. The spectrum of the hydrated electron (not shown) used in the data analysis is taken from ref 25. In the remainder of this work, we implicitly assume that all species are in the aqueous phase unless it is specifically stated otherwise.

III. Experimental Setup

The double-beam transient absorption spectrometer utilized in this work is similar to the one used in a previous study.[26] Briefly, a 1 kHz titanium-sapphire laser system emitting 100 fs pulses with pulse energy of 0.75 mJ is frequency quadrupled to generate the 200 nm pulse used to initiate the photolysis. The ~8 μJ pump pulse is modulated at 0.5 kHz by a mechanical chopper synchronized to the 1 kHz pulse repetition rate and sent through a scanning delay line and a $\lambda/2$ wave plate before it is focused through the sample by a $f = 50$ cm parabolic mirror. The probe pulses covering the spectral range from 460 to 620 nm are generated by a two-stage optical parametric amplifier (OPA) pumped at 400 nm. Probe pulses ranging from 230 to 460 nm are produced by frequency doubling the pulses from the OPA in a 0.2 mm BBO crystal, while the spectral region between 200 and 238 nm is covered by sum frequency mixing the frequency-doubled output from the OPA with residual 800 nm pulses. The probe beam is then split into a signal beam and a reference beam. The signal beam is focused onto the sample by an $f = 10$ cm CaF_2 lens and probes the sample inside the area defined by the pump beam, while the reference beam passes the sample. Signal and reference pulses are then detected by matched photodiodes and boxcar integrators before being processed by a digital lock-in amplifier referenced to the 0.5 kHz modulation of the pump pulse. The time resolution of the spectrometer is 300 fs.

The sample is a ~0.15 mm thick jet of an aqueous solution of HCOOH with a concentration of 1.0 M. At this concentration, formic acid is weakly deprotonated ($pK_a = 3.75$), resulting in a formate ion concentration of ~13 mM. In a separate measurement, we determined that the extinction coefficient at 200 nm of the aqueous formate ion is $\epsilon = 93 \pm 6\ M^{-1}\ cm^{-1}$. Hence, less than 3% of the molecules excited by the pump pulse are formate ions. The concentration of the formic acid dimer is negligible at a 1.0 M concentration of formic acid.[27] The flow was adjusted to give a fresh sample for every laser pulse. No measurable degradation of the solution was observed during the measurements, but to avoid potential accumulation of permanent photoproducts, the solution was replaced regularly. The reproducibility of the transient absorption data was tested among consecutive scans as well as by repeating the measurements on different days using different samples. From numerous measurements, we found that the data could be measured on a common absorption scale with an uncertainty smaller than ±10%. The uncertainties quoted in the remainder of this work refer only to uncertainties pertaining to our measurements, as most referenced spectral data are reported without error estimates.

IV. Experimental Results

The absorption, $\Delta A(\lambda,t)$, of aqueous HCOOH induced by the 200-nm pump pulse was measured at 0.2 eV intervals in the spectral range from 200 to 400 nm. Common to all curves is

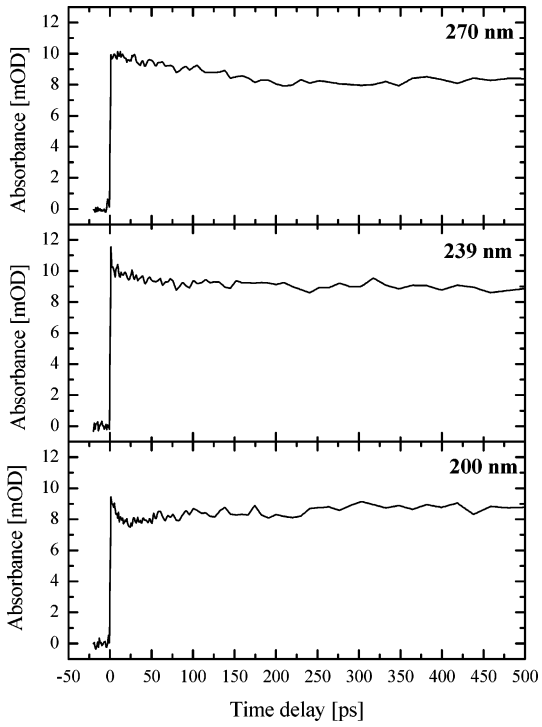

Figure 2. Transient absorption at three different probe wavelengths following the 200 nm pump pulse. The transient absorption was obtained at orthogonal pump−probe polarization. At 270 nm, the transient shows the dynamics of only the OH radical formed in the photolysis. At 200 nm, the bleaching of the formic acid causes the slow rise of the signal after an initial fast decay. The transient at 239 nm contains both contributions.

an initial sharp peak, which originates from the coherent absorption of one pump and one probe photon in water.[28] On the basis of the prompt response of the two-photon absorption signal, we take the position and width of these peaks to mark the point of zero delay and temporal resolution (300 fs), respectively. The two-photon ionization of water produces hydrated electrons, which absorb from the vacuum ultraviolet to far into the infrared part of the spectrum.[29] The contribution from the hydrated electrons has been determined from absorption transients measured between 400 and 620 nm (not shown). On the basis of the good agreement with the spectral and temporal signatures of the hydrated electron, together with the quadratic intensity dependence of the signal at 620 nm, we infer that photoproducts others than the hydrated electron contribute no more than 0.3 mOD in the region from 400 to 620 nm. The absorption pertaining to hydrated electrons is subtracted from the data presented here. Separate measurements at 213 nm showed a linear intensity dependence of the induced absorption, thus confirming that the measured absorption transient originate from one-photon excitation of formic acid. At a 213 nm probe wavelength, we measured the transient absorption for both parallel and perpendicular pump−probe polarizations. The data obtained were identical within the experimental uncertainty, thus showing no sign of rotational anisotropy.

In Figure 2, we show the characteristic time evolution at three selected wavelengths. At 270 nm, the induced absorption rises to a maximum within 0.3 ps and subsequently decays slowly on a time scale of several hundred picoseconds. The absorption transient at 239 nm is nearly featureless except for the slow decay also observed at long probe wavelengths. At 200 nm, the dynamics is more complex: After an instrument-limited rise, a minor fraction of the absorption decays on a 20 ps time scale. Simultaneously, a second component rises slowly on a 100 ps time scale, and after 200 ps, the transient absorption stays constant to 500 ps, which is the longest delay attainable with our experimental setup.

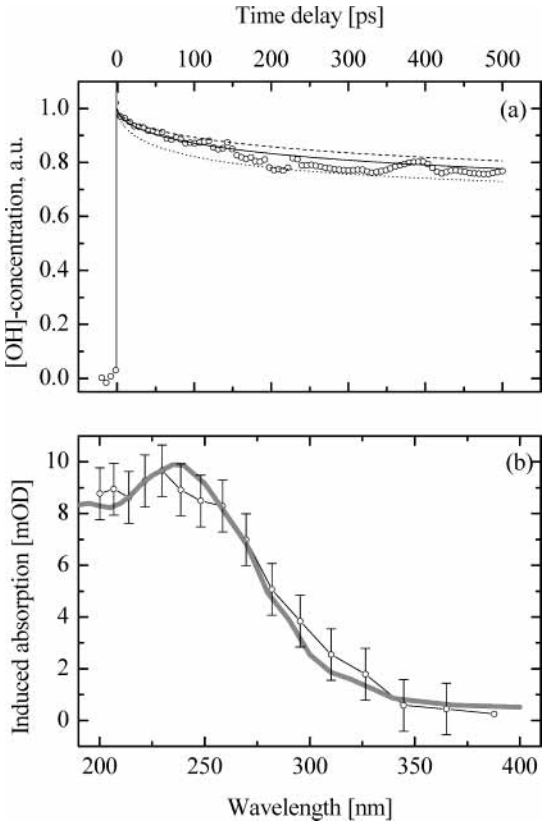

Figure 3. (a) Time evolution of the OH concentration obtained by spectrally integrating the measured transient absorption from 250 to 400 nm. (b) At long delay times, the transient spectrum, including the bleaching contribution from HCOOH, shows excellent agreement with the spectra of OH and HCOOH shown in Figure 1.

The spectral shape of the induced absorption from 250 to 400 nm closely resembles the absorption spectrum of OH(aq), and additionally, all of the transients in this range show the same temporal evolution. Figure 3a shows the time evolution obtained when the transient absorption signal is spectrally integrated from 250 to 400 nm. The induced absorption decays with a time constant of 130 ps to a plateau of 75% of the peak absorption. After 250 ps, the transient absorption is nearly constant, and by averaging the induced absorption from 250 to 500 ps, we obtain the spectrum depicted in Figure 3b. The full line corresponds to the expected induced absorption spectrum assuming that 1.1 mM HCOOH is photolyzed to HCO + OH *and* that *no* transient absorption by the formyl radical formed in the photolysis occurs. The good agreement with the absorption spectrum of OH indicates that photolytic formation of OH is the dominant primary product channel following photolysis of HCOOH at 200 nm and that the OH concentration decays as indicated in Figure 3a.

V. Discussion

The experimental data thus show that OH is the dominant product among the species absorbing in the investigated spectral range. The formation of OH is accompanied by HCO, which, according to gas-phase measurements, exhibits a relatively strong absorption band peaking at 230 nm. However, detailed analysis shows that the transient absorption data are not compatible with the HCO gas-phase absorption spectrum. Thus, to comply with the experimental data, the HCO(aq) absorption

TABLE 2: Vertical Excitation Energies (Δ/eV) and Oscillator Strengths (*f*) for the Transition from the Ground State to the Lowest Electronic States for the Isomers [HCO, nH_2O] and [$HC(OH)_2$, $(n-1)H_2O$][a]

		[HCO, nH_2O]				[$HC(OH)_2$, $(n-1)H_2O$]			
n	method[b]	Δ_1	f_1	Δ_2	f_2	Δ_1	f_1	Δ_2	f_2
0	CIS/aug-cc-pVDZ	2.73	0.002	6.88	0.043	–	–	–	–
	CIS(D)/aug-cc-pVDZ	2.40	–	5.47	–				
	CCSD/aug-cc-pVDZ	2.20	0.001	5.42	0.032				
	CCSD/aug-cc-pVTZ	2.17	0.001	5.59	0.032				
	CCSD/aug-cc-pVQZ	2.17	0.001	5.65	0.032				
1	CIS/aug-cc-pVDZ	2.73	0.002	7.33	0.024	5.61	0.007	6.33	0.002
	CIS(D)/aug-cc-pVDZ	2.39	–	5.79	–	3.94	–	4.55	–
	CCSD/aug-cc-pVDZ	2.20	0.001	5.75	0.022	3.80	0.004	4.80	0.006
4	CIS/aug-cc-pVDZ	3.29	0.004	7.10	0.024	5.97	0.005	6.49	0.009
	CIS(D)/aug-cc-pVDZ	2.91	–	5.69	–	4.22	–	4.66	–
8	CIS/aug-cc-pVDZ	3.65	0.006	7.22	0.021	6.17	0.016	6.97	0.005
	CIS(D)/aug-cc-pVDZ	3.22	–	5.51	–	4.45	–	4.99	–
9	CIS/aug-cc-pVDZ	2.96	0.003	7.66	0.010	–	–	–	–
	CIS(D)/aug-cc-pVDZ	2.58	–	5.80	–	–	–	–	–

[a] Structures of the isomers derived from density functional calculations B3LYP/6-31G(d). [b] CIS and CIS(D) calculations were done using Gaussian 03, and the CCSD calculations were done using the AcesII program system[41] and the excitation energy implementation of ref 42.

spectrum must either be very weak or, alternatively, be blue shifted below 200 nm as a result of the hydration. In an attempt to quantify the effect of hydration, we performed theoretical calculations on HCO and hydrated HCO clusters. Calculations were performed at the three levels configuration interaction singles (CIS), CIS with a perturbative doubles correction [CIS(D)], and coupled-cluster singles and doubles (CCSD) using extended basis sets. The calculated excitation energies are listed in Table 2. The CIS(D) and CCSD results are very similar for HCO and [HCO, $1H_2O$] in terms of both absolute values and the shift upon hydration, adding support to the accuracy of the CIS(D) method for the particular structures used. The agreement of the calculations with the experimental gas phase band maxima around 2.2 and 5.4 eV is as good as can be expected, i.e., within a few tenths of an electronvolt for CCSD. However, even though addition of a single water molecule causes a significant increase in excitation energy, proceeding with CIS(D) to larger clusters does not continue this trend, and the cluster calculations provide no clear evidence for a major shift in the excitation energy. We are thus left with two possibilities: (i) the use of limited-size energy-optimized clusters with the available electronic structure methods does not provide an adequate description of the excitations in HCO(aq) or (ii) the absence of HCO absorption can be explained by HCO having undergone further fast reactions to products, causing no absorption that can be detected in the present experimental setup. We have investigated two mechanisms to probe the latter possibility. First, we consider a fast reaction of HCO with solvent molecules. The initial excess energy is equally split between the two fragments as kinetic energy. For many orientations of HCO relative to neighboring solvent molecules the energy is sufficient to overcome the barrier for the process $HCO + H_2O \rightarrow HC(OH)_2$. We estimated the barrier height by calculating the activation energy for converting a selected conformer of [HCO, $4H_2O$] into [$HC(OH)_2$, $3H_2O$]. Using density functional theory at the B3LYP/6-311+G(d,p) level, we calculate the activation energy to be 80 kJ/mol for the cluster alone and 73 kJ/mol when the cluster is embedded in a polarizable continuum using PCM theory.[30] The two conformers and the transition state are depicted in Figure 4. It appears from this figure that the energy of the [$HC(OH)_2$, $3H_2O$] conformer is only 4 kJ/mol lower than that of the [HCO, $4H_2O$] conformer, which would indicate that the two species would coexist in equilibrium. However, the use of a small number of solvent molecules in energy-optimized structures is unlikely to give an adequate representation of the hydrogen-bond network, especially for a species with two hydroxyl groups. Preliminary investigations [B3LYP/6-31G(d) level] of clusters with eight water molecules show that the energy for [$HC(OH)_2$, $7H_2O$] is about 20 kJ/mol lower than of [HCO, $8H_2O$], suggesting that $HC(OH)_2$ might be the dominant species in bulk water. The UV absorption spectrum of $HC(OH)_2$ is unknown. Theoretical calculations along similar lines as for HCO are included in Table 2. They indicate that $HC(OH)_2$ has several weakly absorbing excited states between 200 and 300 nm. Additional sources of absorption at these wavelengths cannot be assigned in the experimental data. This suggests that this reaction is not dominant at short times or that the absorption is so weak and broad that it cannot be detected.

Second, we consider an ionization-mediated mechanism to explain the absence of the HCO(aq) signal, i.e., [HCO, nH_2O] $\rightarrow$ [HCO, nH_2O]$^+ + e^-$. The ionization energy for the HCO molecule to form the linear singlet HCO^+ ion in the gas phase is 8.12 eV. This energy is lowered substantially in the aqueous phase because of solvation of the charges and because the [HCO, nH_2O]$^+$ cluster ($n > 1$) readily rearranges to a formic acid complex [HCOOH, H_3O^+, $(n-2)H_2O$]. The energy of this complex relative to that of [HCO, nH_2O] in aqueous solution is estimated using PCM theory[30] on geometry-optimized clusters at the B3LYP/6-31G(d) level. For $n = 4$ and $n = 9$, we find 186.0 and 184.4 kJ/mol, respectively. Considering that the hydration energy for the electron is about 150 kJ/mol, we estimate that the energy requirement for the above ionization is about 35 kJ/mol, which is available from the excess energy of the HCO fragment. However, the mechanism predicts that the concentrations of electrons and OH radicals should be the same, which is at variance with the observation of the concentration of solvated electrons following the photolysis pulse. In summary, we have not found any clear explanation for the absence of the absorption from the HCO produced along with the OH in the photodissociation of formic acid in water.

From Figure 3, we observe that the concentration of the OH radical decays with a time constant of 130 ps to a constant level of approximately 75% of the original concentration of OH. To test whether the decay of the OH concentration is caused by geminate diffusive recombination,[31] we solved the spherically symmetric diffusion problem (SSDP).[31,32] This requires knowledge of the sum of the diffusion constants of the geminate partners, the initial fragment distribution, the contact radius, the interaction potential between the fragments, and the rate of reaction at the contact radius. The diffusion constant of HCO,

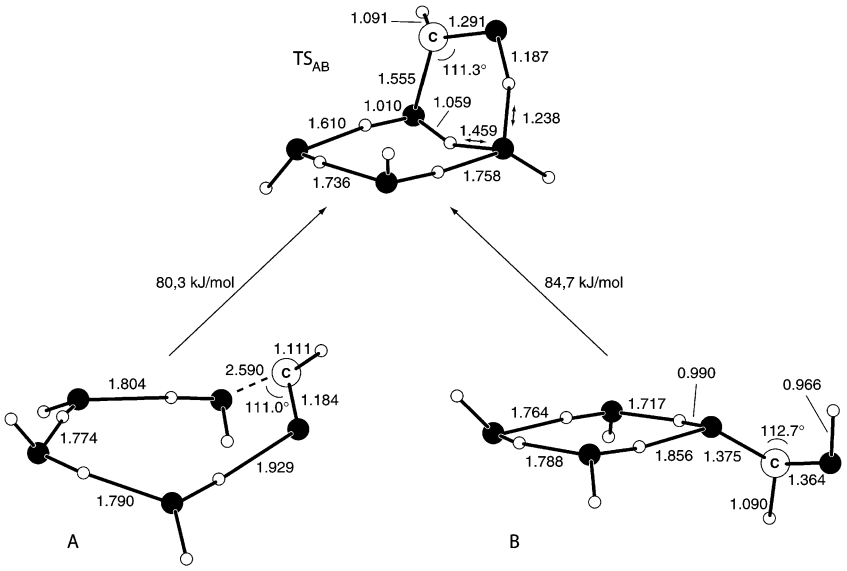

Figure 4. Structures of conformers of (A) [HCO, $4H_2O$] and (B) [$HC(OH)_2$, $3H_2O$] and the transition state (TS_{AB}) that connects them. The structures are calculated at the B3LYP/6-311+G(d,p) level of theory. The distances and angles are in angstroms and degrees, respectively. ● indicates an oxygen atom, and ○ indicates a hydrogen atom. The numbers attached to the arrows refer to the energy separations (kJ/mol) at 0 K of the involved structures. The dominant motion in the conversion mode of the transition state is an asymmetric stretch of two OH bonds marked by a double-headed arrow.

or alternatively $HC(OH)_2$, is not known, but because the diffusion constant of OH is large ($D_{OH} = 2.2 \times 10^5$ cm^2 s^{-1}),[33] we assume that D_{OH} will dominate. The fragment distribution after the photolysis is represented by an exponentially decaying distribution with a characteristic length in the range between 0.5 and 1.0 nm. The fragment distribution is quite wide as a result of the large kinetic energy release.[31] Because both fragments are neutral, we set the interaction potential equal to zero. The contact radius is varied between 0.5 and 1 nm, which are the approximate radii of the first and second solvation shells, respectively, around the solvated fragments. Because the OH + HCO/$HC(OH)_2$ reaction is a radical−radical recombination, we assume that the recombination rate is diffusion-limited and consequently adopt absorbing boundary conditions at the contact radius. The choice of parameters and boundary conditions is somewhat arbitrary, as the data can be well represented within a wide variety of parameters. This is shown in Figure 3a, where the simulated dynamics of the diffusive recombination is illustrated for a few values of the parameters. Good agreement is observed in terms of both the fraction of OH molecules escaping geminate recombination (∼75%) and the temporal dynamics of the decay ($\tau = 130$ ps). The agreement suggests that, despite the uncertainty concerning the fate of the HCO radical, a geminate partner with which the OH radical can recombine remains. The observed time scale for recombination and the fraction of molecules escaping are in accordance with the recent observations of OH recombination following photolysis of H_2O_2 at 200 nm.[34] In this experiment, Crowell et al. inferred a slow release of OH radicals from the solvent cage prior to the geminate recombination. This process takes place with a time constant of 29 ps. Although not easily detectable in our experiment, we cannot rule out that the same process is taking place following the photolysis of HCOOH.

To investigate whether additional channels are open in the UV photolysis of formic acid, we subtracted the transient absorption pertaining to the OH radical from the experimental data from 200 to 400 nm. The spectral shape of the OH signal, including the negative contribution from the HCOOH molecules and the temporal evolution of this signal, is obtained from Figure 3a,b. Thereby, we obtain the residual transient absorption caused by all channels other than the OH channel. As the residual transient absorption is weak, we averaged the signal over both time and wavelength. When averaged over time, from 0 to 250 ps, we find the spectral shape of the residual absorption, Figure 5a, to be very similar to the absorption spectrum of ground-state formic acid, also shown in Figure 5a. Note that the residual transient absorption is purely negative. This suggests that, apart from the OH + HCO channel, the only other open channel corresponds to the excitation of formic acid into a "dark channel", causing little or no absorption between 200 and 620. When the residual transient absorption is spectrally averaged from 200 to 400 nm, we obtain the temporal dynamics depicted in Figure 5b. This shows that the dark channel decays to ground-state formic acid with a time constant of ∼170 ps. From the amplitude of the residual transient absorption before the spectral and temporal averaging, we estimate that 75% of the excited formic acid molecules populate the dark channel and that the rest, 25%, dissociate to the OH channel. From the OH channel, 25% of the pairs recombine to form HCOOH, and the remaining 75% escape diffusive geminate recombination. If the residual transient is analyzed in detail, there is a weak spectral development of the transient, and most notably, the peak residual absorption is delayed (15−20 ps) relative to $t = 0$ defined by the pump pulse. This is evident from Figure 5b, where the temporal dynamics is flat in the first 20 ps. This is a signature that could indicate that the release of the OH radical from the solvent cage is not instantaneous,[34] as was assumed in the above analysis.

There are several candidates that can explain the dark channel described above: it could be formic acid dissociated into CO + H_2O or CO_2 + H_2, vibrationally excited formic acid, or a long-lived triplet state of formic acid. When gas-phase formic acid molecules are photolyzed with UV light, a substantial fraction dissociate to CO + H_2O or CO_2 + H_2 via internal conversion from the photoexcited S_1 state to the vibrationally hot S_0 ground state.[4] The dissociation then proceeds from the electronic ground state to form CO or CO_2. The same excitation of the S_1 state and rapid internal conversion is likely to occur

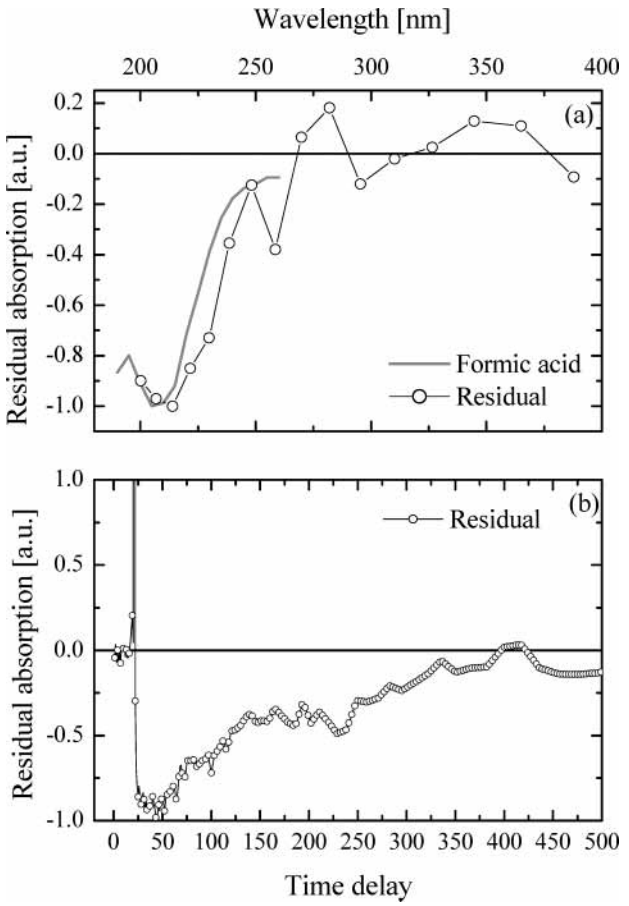

Figure 5. Residual transient absorption obtained after subtracting the contributions from the induced absorption of the OH radical and the induced bleaching of HCOOH. The residual spectrum (—○—) is similar to the static spectrum of HCOOH (—), indicating that a substantial fraction of the HCOOH molecules are excited into dark states with little or no absorption in the spectral range of the probe pulses.

in the condensed phase, but the vibrational relaxation of the S_0 ground state is expected to be much faster in liquid water. The vibrational relaxation can quickly reduce the energy of the S_0 state below the threshold for the dissociation and effectively close those of the CO + H_2O and CO_2 + H_2 channels. The decay of the residual transient absorption could be interpreted as vibrational relaxation of the formic acid molecules.[35,36] However, a vibrational relaxation time of 170 ps for a polar molecule in a polar liquid would be unusually slow. The vibrational relaxation time of formic acid is expected to be well below 10 ps.[26,37−39] Furthermore, the spectral shift and broadening usually accompanying vibrational relaxation are not observed. Alternatively, if the CO + H_2O and CO_2 + H_2 channels are open, then the 170-ps time decay time could correspond to the geminate recombination time for products. However, this possibility can be excluded because calculations indicate reaction barriers on the order of ∼285−300 kJ/mol,[40] which effectively eliminate fast geminate recombination between CO + H_2O and CO_2 + H_2. Finally, there is the possibility that the dark channel is caused by excitation or intersystem crossing into the triplet states of formic acid with an absorption spectrum outside the spectral range covered by the probe pulses. In this case, the 170-ps decay time would correspond to the lifetime of the triplet state in solution. The population of such a triplet state is in accordance with the observation that the main photolytic product is the OH radical. Calculations[4] on gas-phase HCOOH show that the dissociation into the HCO + OH channel can take place on either the S_1 or T_1 state. Unfortunately, most of these considerations are rather speculative as the very low extinction coefficient of formic acid precludes a detailed experimental investigation of the nature of the dark channel. We can, however estimate maximum contributions from the other detectable channels listed in Table 1. The contributions from channels corresponding to dissociation of a hydrogen atom (H + COOH or H + HCOO) can be limited to less than 5% because of the large extinction of the reaction products.

In conclusion, we have investigated the primary photolytic processes of aqueous formic acid using femtosecond transient absorption spectroscopy. We find that 25% of the formic acid molecules excited by the 200 nm pump pulse dissociate to produce the OH radical and the remaining 75% return to the formic acid ground state with a time constant of 170 ps. The photolytic products were probed in the wavelengths range from 200 to 620 nm with 200 fs time resolution. Using electronic structure calculations, we investigated a number of possible reaction schemes involving the OH radical and the (hydrated/ionized) formyl radical in an attempt to understand the absence of a detectable signal from the (hydrated) formyl radical. A fraction of the OH radicals (∼25%) recombine through diffusive geminate recombination with the (hydrated) formyl radical on a 100 ps time scale.

References and Notes

(1) Jorissen, A.; Cerf, C. *Origins Life Evol. Biosphere* **2002**, *32*, 129−142.
(2) Adams, G. E.; Hart, E. J. *J. Am. Chem. Soc.* **1962**, *84*, 3994.
(3) Karpel, N.; Leitner, V.; Dore, M. *New J. Chem.* **1995**, *19*, 1171−1176.
(4) He, H.-Y.; Fang, W.-H. *J. Am. Chem. Soc.* **2003**, *125*, 16139−16147.
(5) Langford, S. R.; Batten, A. D.; Kono, M.; Ashfold, M. N. R. *J. Chem. Soc., Faraday Trans.* **1997**, *93*, 3757−3764.
(6) Su, H. M.; He, Y.; Kong, F. N.; Fang, W. H.; Liu, R. Z. *J. Chem. Phys.* **2000**, *113*, 1891−1897.
(7) Brouard, M.; Simons, J. P.; Wang, J. X. *Faraday Discuss.* **1991**, 63−72.
(8) Ebata, T.; Fujii, A.; Amano, T.; Ito, M. *J. Phys. Chem.* **1987**, *91*, 6095−6097.
(9) Lee, K. W.; Lee, K. S.; Jung, K. H.; Volpp, H. R. *J. Chem. Phys.* **2002**, *117*, 9266−9274.
(10) Brouard, M.; Wang, J. X. *J. Chem. Soc., Faraday Trans.* **1992**, *88*, 3511−3516.
(11) Lundell, J.; Rasanen, M. *J. Mol. Struct.* **1997**, *437*, 349−358.
(12) Khriachtchev, L.; Macoas, E.; Pettersson, M.; Rasanen, M. *J. Am. Chem. Soc.* **2002**, *124*, 10994−10995.
(13) Tabayashi, K.; Aoyama, J.; Matsui, M.; Hino, T.; Saito, K. *J. Chem. Phys.* **1999**, *110*, 9547−9554.
(14) Singleton, D. L.; Paraskevopoulos, G.; Irwin, R. S. *Res. Chem. Intermed.* **1989**, *12*, 1−12.
(15) Pagsberg, P.; Christen, H.; Rabani, J.; Nilsson, G.; Fenger, J.; Nielsen, S. O. *J. Phys. Chem.* **1969**, *73*, 1029.
(16) Boyle, J. W.; Ghormley, J. A.; Hochanad, C. J.; Riley, J. R. *J. Phys. Chem.* **1969**, *73*, 2886.
(17) Hochanadel, C. J.; Sworski, T. J.; Ogren, P. J. *J. Phys. Chem.* **1980**, *84*, 231−235.
(18) Park, H. R.; Getoff, N. *J. Photochem. Photobiol. A: Chem.* **1988**, *43*, 155−163.
(19) Nielsen, S. O.; Pagsberg, P.; Rabani, J.; Christen, H.; Nilsson, G. *Chem. Commun.* **1968**, 1523.
(20) Neta, P.; Simic, M.; Hayon, E. *J. Phys. Chem.* **1969**, *73*, 4207.
(21) Mittal, L. J.; Mittal, J. P.; Hayon, E. *J. Phys. Chem.* **1973**, *77*, 2267−2273.
(22) Ebert, M., Keene, J. P., Swallow, A. J., Eds. *Pulse Radiolysis*; Academic Press: London, 1966.
(23) Crowell, R. A.; Bartels, D. M. *J. Phys. Chem.* **1996**, *100*, 17940−17949.
(24) Thomsen, C. L.; Madsen, D.; Keiding, S. R.; Thøgersen, J.; Christiansen, O. *J. Chem. Phys.* **1999**, *110*, 3453−3462.
(25) Boyle, J. W.; Riley, J. F.; Ghormley, J. A.; Hochanad, C. J. *Radiat. Res.* **1967**, *31*, 582.
(26) Madsen, D.; Larsen, J.; Jensen, S. J. K.; Keiding, S. R.; Thøgersen, J. *J. Am. Chem. Soc.* **2003**, *125*, 15571−15576.

(27) Zarakhini, N. G.; Vinnik, M. I. *Zh. Fiz. Khim.* **1963**, *37*, 2550−2553.
(28) Thomsen, C. L.; Madsen, D.; Keiding, S. R.; Thøgersen, J.; Christiansen, O. *J. Chem. Phys.* **1999**, *110*, 3453−3462.
(29) Madsen, D.; Thomsen, C. L.; Thøgersen, J.; Keiding, S. R. *J. Chem. Phys.* **2000**, *113*, 1126−1134.
(30) Tomasi, J.; Persico, M. *Chem. Rev.* **1994**, *94*, 2027−2094.
(31) Madsen, A.; Thomsen, C. L.; Poulsen, J. A.; Jensen, S. J. K.; Thøgersen, J.; Keiding, S. R.; Krissinel, E. B. *J. Phys. Chem. A* **2003**, *107*, 3606−3611.
(32) Krissinel, E. B.; Agmon, N. *J. Comput. Chem.* **1996**, *17*, 1085−1098.
(33) Elliot, A. J.; Mccracken, D. R.; Buxton, G. V.; Wood, N. D. *J. Chem. Soc., Faraday Trans.* **1990**, *86*, 1539−1547.
(34) Crowell, R. A.; Lian, R.; Sauer, M. C.; Oulianow, D. A.; Shkrob, I. A. *Chem. Phys. Lett.* **2003**, *383*, 481−485.
(35) Poulsen, J. A.; Thomsen, C. L.; Keiding, S. R.; Thøgersen, J. *J. Chem. Phys.* **1998**, *108*, 8461−8471.
(36) Thomsen, C. L.; Thøgersen, J.; Keiding, S. R. *J. Chem. Phys.* **2001**, *114*, 4099−4106.
(37) Lock, A. J.; Woutersen, S.; Bakker, H. J. *J. Phys. Chem. A* **2001**, *105*, 1238−1243.
(38) Owrutsky, J. C.; Raftery, D.; Hochstrasser, R. M. *Annu. Rev. Phys. Chem.* **1994**, *45*, 519−555.
(39) Poulsen, J.; Keiding, S. R.; Rossky, P. J. *Chem. Phys. Lett.* **2001**, *336*, 488−494.
(40) Khriachtchev, L.; Macoas, E.; Pettersson, M.; Rasanen, M. *J. Am. Chem. Soc.* **2002**, *124*, 10994−10995.
(41) Stanton, J. F.; Gauss, J.; Watts, J. D.; Lauderdale, W. J.; Bartlett, R. J. *Int. J. Quantum Chem.* **1992**, 879−894.
(42) Stanton, J. F.; Bartlett, R. J. *J. Chem. Phys.* **1993**, *98*, 7029−7039.